

**Fig. 1.** Antibiotic elimination during HTC. (A) Temperature dynamics during the process, the hollow square represents the sampling point. (B) Concentration of antibiotics detected in the initial mixture. (C) Removal efficiency of antibiotics during composting.

## 1. Introduction

Worldwide emergence and rapid spread of antimicrobial resistance (AMR) among humans, animals, and environments is widely acknowledged as a complex "One Health" challenge [1]. Sewage sludge has been identified as a hotspot of antibiotic residues and antibiotic resistance genes (ARGs) [2]. However, conventional composting, despite its established use in sludge disposal, has limitations in effective removal of these emerging contaminants [3,4], which raises concerns about their potential dissemination in soil-plant systems through land application [5,6]. Consequently, it is imperative to explore more efficient composting technologies for the elimination of antibiotics and ARGs.

Hyperthermophilic composting (HTC), known for its capability in degrading organic contaminants and removing ARGs [7], has emerged as a promising approach for solid waste treatment and recycling [8]. Previous studies have showed efficient removal of 27 ARGs compared to conventional composting and revealed the crucial roles of high composting temperature and significant reduction of the mobile genetic elements (MGEs) in ARG elimination [9,10]. However, there is a lack of studies that examine simultaneous removal of antibiotic residues and

ARGs in hyperthermophilic sludge composting. A more comprehensive evaluation of antibiotics and ARGs encompassing a broader range is also needed, considering the complex contamination situation in sewage sludge [11].

The underlying mechanisms of antibiotic elimination by HTC are not fully explored yet. Previous study tentatively ascribed the near-complete removal of tylosin to degradation under high-temperature condition [10]. While, a study comparing antibiotic removal in manure composting at 60°C and 30°C suggested that elevated temperature did not universally facilitate antibiotic degradation [12]. In addition to temperature dependent abiotic processes such as volatilization and adsorption [13], biodegradation has been considered a primary pathway for antibiotic dissipation during composting [14]. However, the declined bacterial diversity and richness during HTC [9,10] further raise concerns about their significance in antibiotic removal under hyperthermophilic conditions. Investigating the roles of microbes in antibiotic elimination during HTC is thus necessary for comprehensive understanding the mechanisms that will provide important theoretical basis for the future application of bioaugmentation and biostimulation technologies in optimizing this process.

Ensuring the quality of compost is of paramount importance for its application [15]. However, in the context of HTC, the comprehensive evaluation of product quality remains inadequate. Typically, compost quality revolves around achieving a high degree of maturity, characterized by sufficient decomposition and the absence of phytotoxic compounds and pathogens [16]. While fecal coliform monitoring has been established, the potential survival and proliferation of various human pathogens during composting also necessitate to be attended [17,18]. A more rigorous safety and quality examination of HTC products is warranted for field application.

To address these questions, a plant-scale HTC of sewage sludge was systematically investigated, where we conducted a comprehensive characterization of the temporal variation in physicochemical properties, antibiotic residues, bacterial communities, and ARG profiles during the process. The aims of this study are (1) to assess the quality of the compost product and the potential of the HTC technique in the elimination of antibiotic, antibiotic resistome and potential human pathogens, (2) to reveal the relationship between the dissipation of antibiotics and HTC bacterial communities, and (3) to decipher the abiotic and biotic factors contributing to ARG variation in HTC and to elucidate the mechanisms underlying their elimination.

## 2. Materials and methods

### 2.1. Hyperthermophilic composting operation and sample collection

The HTC was conducted in December at a full-scale hyperthermophilic composting plant located in Xiamen, China. The plant comprised a series of open concrete cells with a size of 3 m × 15 m × 8 m (height × width × length) in the indoor facility area, where the organic waste was piled up and composted at an average ambient temperature ranging from 20<sup>o</sup> C to 25<sup>o</sup> C.

In this study, approximately 100 tons of dewatered sewage sludge (with a moisture content of 78 %) from Huli Wastewater Treatment Plant (Huli WWTP, Xiamen, China) was mixed with the okara and seafood waste from local farms in a ratio of 8:1:1 (w:w:w). Composting end-products from the last batch was added as inoculating agent and bulking agents. Based on previous experience [9,19], the initial moisture content and C/N ratio of the compost mixture were adjusted to 60 % and 9, respectively, to achieve effective hyperthermophilic composting.

The composting process lasted for 46 days with periodical mechanical turning of the compost mixture every 7 days using a forklift to adjust the aeration condition. Daily temperature was monitored using an automatic thermometer. The initial temperature inside the pile was 53<sup>o</sup> C, which increased rapidly within 5 days. After six cycles of periodic temperature change (ranging from 60 to 95<sup>o</sup> C), considered as a prolonged thermophilic phase, the composting process ended with a cooling and maturation phase for 4 days (Fig. 1A).

Samples were collected on day 0, 4, 8, 12, 20, 32, and 46, as indicated in Fig. 1A, representing three stages of the process: (i) the early composting, including initial mixture and calefactive phase of composting (D0 and D4); (ii) the mid phase, referred to the major period of thermophilic phase (D8, D12 and D20); (iii) the late phase, including end of thermophilic phase and final product of composting (D32 and D46). Five hundred grams of samples were collected and kept in brown glass jars to prevent the adsorption and photodegradation of antibiotics. Each sample was divided into two portions, with one stored at -20<sup>o</sup> C for DNA extraction, and the other at 4<sup>o</sup> C for physicochemical analysis.

### 2.2. Physicochemical characterization and phytotoxicity test

Electrical conductivity (EC) and pH were examined using a pH-EC meter (Accumet® Excel XL60, Fisher Scientific Inc., USA) in a 1:10 (w/v) water-soluble extract. The moisture content and organic matter content (OM) were determined by calculating the mass loss of the aliquots upon heating the samples in an oven at 105<sup>o</sup> C for 24 h and a muffle

furnace at 550<sup>o</sup> C for 2 h, respectively. The dissolved organic carbon (DOC) was extracted with 0.5 M K<sub>2</sub>SO<sub>4</sub> and then analyzed using a multi N/C 2100 TOC/TN analyzer (Analytik Jena, Jena, Germany) [20]. Inorganic nitrogen content (NO<sub>3</sub>-N, NO<sub>2</sub>-N, and NH<sub>4</sub>-N) were extracted with ddH<sub>2</sub>O at a ratio of 1:10 (w/v) and measured using ion chromatography (ICS-3000; Dionex, Sunnyvale, CA, USA) [21]. The nitrification index (NI) was calculated as the ratio between ammonium and nitrate content. Total carbon (TC) and total nitrogen (TN) were determined using an element analyzer (Vario MAX C/N/S; Elementar) to calculate the C/N ratio. Potential phytotoxicity of the compost product was evaluated using seed germination index (GI) following the method described by Guo et al. [22].

### 2.3. Antibiotic analysis

Concentrations of twenty-seven antibiotics were determined using the internal standard method, including four tetracyclines (TCs): chlortetracycline (CTC), doxycycline (DOC), oxytetracycline (OTC), and tetracycline (TTC); eleven sulfonamide compounds (SAs, including synergist trimethoprim): sulfadiazine (SDZ), sulfamethoxazole (SMX), sulfamethazine (SMZ), sulfamerazine (SMR), sulfamonomethoxine (SMM), sulfaquinoxaline (SQX), sulfadimethoxine (SDM), sulfamer (SME), sulfaclozine (SCZ), sulfathiazole (STZ), and trimethoprim (TMP); five fluoroquinolones (FQs): ciprofloxacin (CFC), danofloxacin (DFC), enrofloxacin (EFC), norfloxacin (NFC), and ofloxacin (OFC); three macrolides (MLs): erythromycin-H<sub>2</sub>O (ETM), roxithromycin (RTM), and tylosin (TLS); three chloramphenicols (CPs): chloramphenicol (CAP), florfenicol (FFC), and thiamphenicol (TPC); one lincocin (LC): lincomycin hydrochloride (LIM).

The sample preparation, extraction, and analysis were conducted following a previous protocol with the modification of an increased sample usage of 0.5 g [23]. The concentrated antibiotics were simultaneously quantified using ultra-performance liquid chromatography-tandem mass spectrometry coupled with a triple quadrupole tandem mass spectrometer (UPLC-MS/MS, AB Sciex 6500, USA).

The removal efficiency of the antibiotic during composting was estimated as follows:

$$RE(\%) = \left(1 - \frac{C_t}{C_0}\right) \times 100$$

where C<sub>0</sub> represent the initial concentration of the antibiotic (ug/kg dry matter), C<sub>t</sub> is the antibiotic concentration for each sample at day *t* during the process.

### 2.4. DNA extraction

The sample (0.5 g) was frozen with liquid nitrogen and grinded prior to DNA extraction using DNeasy PowerLyzer PowerSoil Kit (Qiagen, Hilden, Germany). The extracted DNA was quantified using a Qubit 3.0 fluorometer (Invitrogen) and stored at -20<sup>o</sup> C for further experiments.

### 2.5. High-throughput quantitative PCR of ARGs and potential human pathogens

Quantification of the ARGs (including MGEs) and potential pathogens were conducted by high-throughput quantitative PCR (HT-qPCR) using a Wafergen SmartChip real-time PCR system (Warfergen, USA) [24,25]. The relative abundance of ARGs and MGEs were determined using a cluster of primer sets targeting 309 ARGs conferring resistance to major classes of antibiotics, 57 MGEs, and 16 S rRNA gene (Table S1) [25]. The reaction system was as previously reported with a detection limit set at a threshold cycle of 31 [26]. Three technical replicates were conducted for each sample, and amplification was considered positive only when all replicates were detected. The absolute copy numbers of

**Table 1**  
The quality of the final product of HTC.

Index Parameters	Measurement Value	Standard	Regulation References
pH	7.9	5.5 –8.5	People's Republic of China agricultural industry standard (NY/T 525–2021)
EC	3.82 mS/cm	< 4 mS/cm	[32]
moisture content	< 30 %	< 40 %	Spanish regulation (BOE 999/2017)
OM	52.3 %	> 35 %	Spanish regulation (BOE 999/2017)
C/N ratio	10	< 20	[33]
NI	0.1	< 0.5	[34]
GI	102 %	> 50 %	[34]

ARGs and MGEs in compost sample was calculated according to Su et al. [3]. Pathogens were quantified using 68 marker genes targeting 33 human pathogens associated with infections in the cornea, intestine, and respiratory system according to our previous study [24].

## 2.6. Bacterial community composition and function prediction

To investigate the composition of bacterial community, the V4 region of 16 S rRNA gene was amplified using the barcoded primer sets 515 F/806 R [27]. The purified amplicons were concentrated and sent for high-throughput sequencing on an Illumina HiSeq 2500 platform (Majorbio, Shanghai, China). Feature table of amplicon sequence variants (ASVs) was generated using the DADA2 plugin [28] in QIIME2 (v2020.09). All data generated were deposited in NCBI Sequence Read Archive (SRA) under the accession number PRJNA1122491. Functional potential of compost bacteria was predicted based on the KEGG database through PICRUSt2 [29].

## 2.7. Statistical analysis

Differences between composting samples were assessed using one-way ANOVA in SPSS 22.0 (IBM, USA). Principal coordinate analysis (PCoA), redundancy analysis (RDA) and Adonis test were conducted using R4.4.2 with vegan 2.6–4 and ggplot2 packages [30]. Heatmap was generated using the pheatmap package (<https://cran.r-project.org/web/packages/pheatmap/index.html>). Network analysis was performed employing the *microeco* package, with results subjected to Benjamini-Hochberg False Discovery Rate (FDR) adjustment and visualized in Gephi 0.9.1 [31]. Pearson correlation and Spearman's rank correlation matrix were obtained with psych package (<https://cran.r-project.org/web/packages/psych/index.html>). Structural equation modeling (SEM) analyses were conducted in SPSS Amos 26.0 (IBM, USA). Origin 10.5.112 (OriginLab, USA) was used for generating other graphs. A p-value < 0.05 was considered significant.

## 3. Results

### 3.1. Characterization of composting product

An integrated assessment on end product (sample D46) suggested acceptable maturity of hyperthermophilic composting product (Table 1). The pH of the compost was 7.9, meeting the requirements of the national standard. Although there is no specific limit on compost application regarding electrical conductivity (EC), compost with high EC content could negatively impact crop growth when used in large amounts. The EC value of our compost was 3.82 mS/cm, which falls below the widely recognized threshold of 4 mS/cm. Besides, the compost met the desired criteria with a moisture content below 30 % and an organic matter (OM) content of 52.3 %, surpassing the recommended values of less than 40 % and greater than 35 %, respectively.

The low C/N ratio (< 20), nitrification index (< 0.5), and high GI value of up to 102 % collectively indicate that the product of HTC was biologically stable and mature, and free of phytotoxicity. The changes of physicochemical properties during composting were also provided (Fig. S1).

Complete elimination of tested potential human pathogens was observed after HTC. Three pathogen marker genes, targeting *Staphylococcus aureus*, *S. pneumoniae*, and *Cronobacter* spp., were detected on D0, indicating the presence of pathogen contamination in the raw materials of compost (Fig. S2). Among them, *S. aureus* was found in all three replicates, with an abundance of  $7.1 \times 10^3$ – $1.3 \times 10^4$  copies/g dry matter (DM). *S. pneumoniae* and *Cronobacter* spp. were only detected in one replicate of D0, with an abundance of  $3.6 \times 10^4$  and  $6.3 \times 10^3$  copies/g DM, respectively. The absence of pathogen marker genes in the final compost product (D46) implies that tested potential pathogens were efficiently eliminated during the HTC process.

### 3.2. Removal of antibiotics

Three FQs, six SAs, one CPs, and one LC were detected in the initial compost mixture (D0, Fig. 1B). FQs exhibited the highest residual concentrations in the mixture, with OFC and CFC detected at levels of up to 124.5 and 106.3 ug/kg DM, respectively. As another major class, SAs was detected at concentrations ranging from 0.07 to 6.35 ug/kg DM. TCs and MLs were not detected.

All tested antibiotics were not detected after composting. As shown in Fig. 1C, the first 12 days was the principal stage for the removal of most antibiotics. The elimination rates of different antibiotic classes varied, showing no apparent correlation with their initial concentrations in the compost. The major sulfonamide, SQX and SMM were completely removed after 4 days of HTC, SDM was not detected on D8. Meanwhile, more than 50 % of the remaining SAs were eliminated and were completely removed after the second temperature rise (D12). However, FQs were more recalcitrant than SAs during the composting. Except for the completely removal of CFC after 12 days, OFC and EFC remained detectable until D32. As one of the major antibiotics of the initial composting mixture, the elimination of OFC was less than 20 % before D12. LIM and CAP dissipated after 12 and 32 days, respectively. These results clearly demonstrated that HTC could effectively eliminate antibiotic residues in sludge.

### 3.3. Reduction of ARGs and MGEs during composting

A total of 154 unique ARGs and 26 MGEs were detected in the composting samples. Among the identified ARGs, the most abundant were those conferring resistance to macrolide-lincosamide-streptogramin B (MLS<sub>B</sub>), multidrug, aminoglycoside, and sulfonamide antibiotics. Transposases were found to be the predominant type of MGEs (Fig. 2A).

HTC significantly altered the patterns of ARGs (Fig. 2). PCoA analysis of ARG profiles indicated that the composition of ARGs significantly changed during the composting process (Fig. 2B). Specifically, samples of D32 and D46 clustered together and were separated from the earlier stage samples along PC1, indicating a significant change in ARG patterns after the mid phase. However, no significant change in diversity was observed as shown by the Shannon and inverse Simpson indexes, despite a reduction in ARG richness (Fig. S3).

HTC eliminated ARGs efficiently. Consistent with the absolute abundance of bacteria, the ARG abundance exhibited a general downward trend during the process and decreased by up to 98.8 % in the final compost product (from  $5.5 \times 10^{10}$  copies/g DM to  $6.6 \times 10^8$  copies/g DM, Fig. 2A). The efficacy of HTC in eliminating MGEs was also notable, with an 88.1 % reduction from  $3 \times 10^9$  copies/g DM to  $3.5 \times 10^8$  copies/g DM. The heatmap provides insights into the fate of different types of MGEs and ARGs conferring resistance to various antibiotics, revealed a significant reduction of their absolute abundance during the

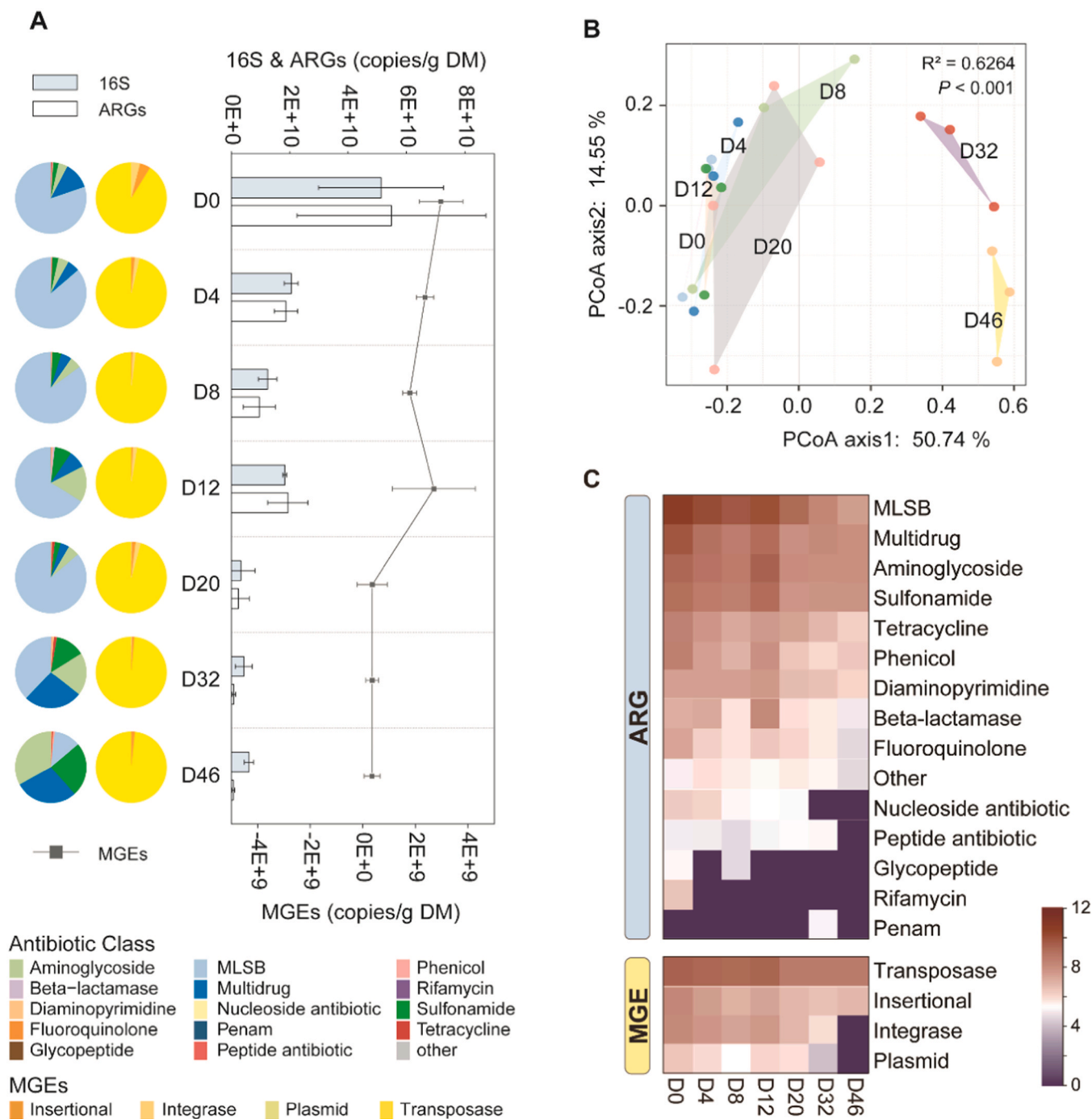


**Fig. 2.** Changes in the distribution profiles of antibiotic resistance during HTC. (A) Temporal changes in absolute copy numbers (copies/g DM) of ARGs and MGEs. The pie charts present the proportion of ARGs and MGEs in compost samples. The stacked columns and line present the sum of absolute copy numbers of 16 S rRNA gene, detected ARGs, and MGEs. (B) The overall distribution pattern of ARGs based on PCoA analysis ordination derived from Bray-Curtis distances. (C) Changes in the absolute abundance of ARGs and MGEs during composting. The abundance was transformed into logarithmic transformation ( $\log_{10}$ ).

HTC (Dunnnett’s test,  $P < 0.05$ ) (Fig. 2C). The absolute abundance of most ARGs, predominantly those conferring resistance to MLSB, multidrug, aminoglycosides, and sulfonamides, significantly decreased from day 0 to day 8 and from day 12 to day 46. Rifamycin and glycopeptide ARGs were completely removed during the mid phase. ARGs resistant to nucleoside antibiotics and peptide antibiotics were completely removed in the late phase, after experiencing the major period of the thermophilic phase, together with penam-resistant ARGs, which were only detected on day 32. Pearson correlation analyses revealed significant correlation between the absolute abundance of ARGs and the concentration of the

corresponding antibiotics ( $r > 0.4$ ,  $P < 0.05$ , Table S2). The absolute abundance of each ARGs and MGEs during composting indicated that the majority of ARGs and MGEs were ultimately eliminated, and only a small fraction of ARGs persisted, particularly multidrug and aminoglycoside resistance genes, and transposases (Detail Fig. S4).

### 3.4. Bacterial community dynamics and functional features

Totally 2180,886 high quality 16 S rRNA gene sequences were obtained, which were clustered into 597 ASVs (ranging from 198 to 504

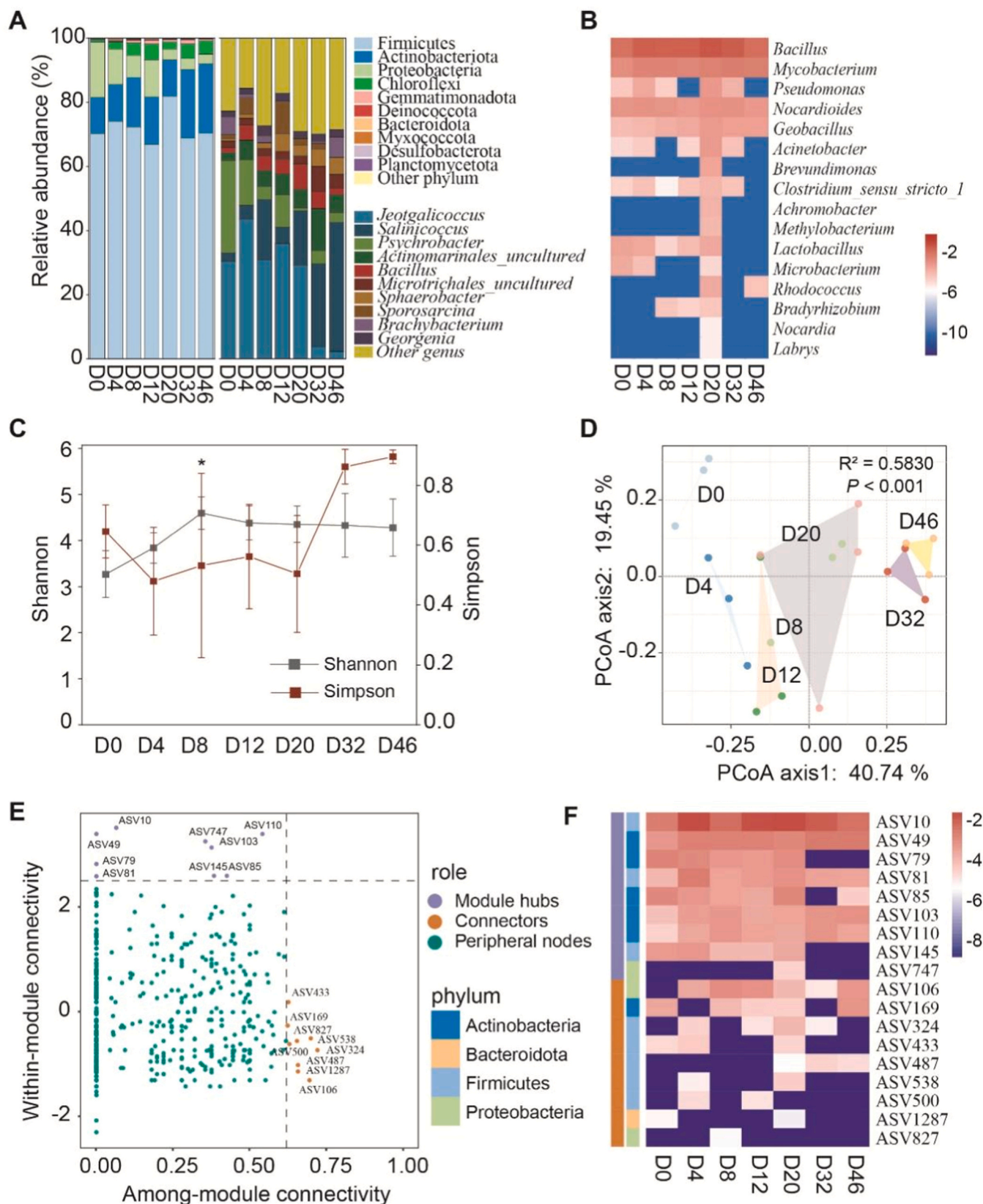


**Fig. 3.** Bacterial community dynamics and co-occurrence patterns during HTC. (A) Taxonomic composition of bacterial communities at the phylum and genus levels. (B) Change in relative abundances of bacterial taxa that predicted to have the capacity for antibiotic degradation based on 16 S rRNA gene amplicon sequencing. (C) Alpha diversity of bacterial communities represented as Shannon and inverse Simpson indexes. Asterisk indicates significant differences compared with D0 (ANOVA analysis followed by post hoc Dunnett's test,  $P < 0.05$ ). (D) PCoA analysis based on the Bray-Curtis distances illustrating the overall distribution pattern of bacterial communities. (E-F) Keystone nodes (E) identified in correlation-based network analysis (based on ASV abundances) for bacterial communities and their abundance changes (F) during composting.

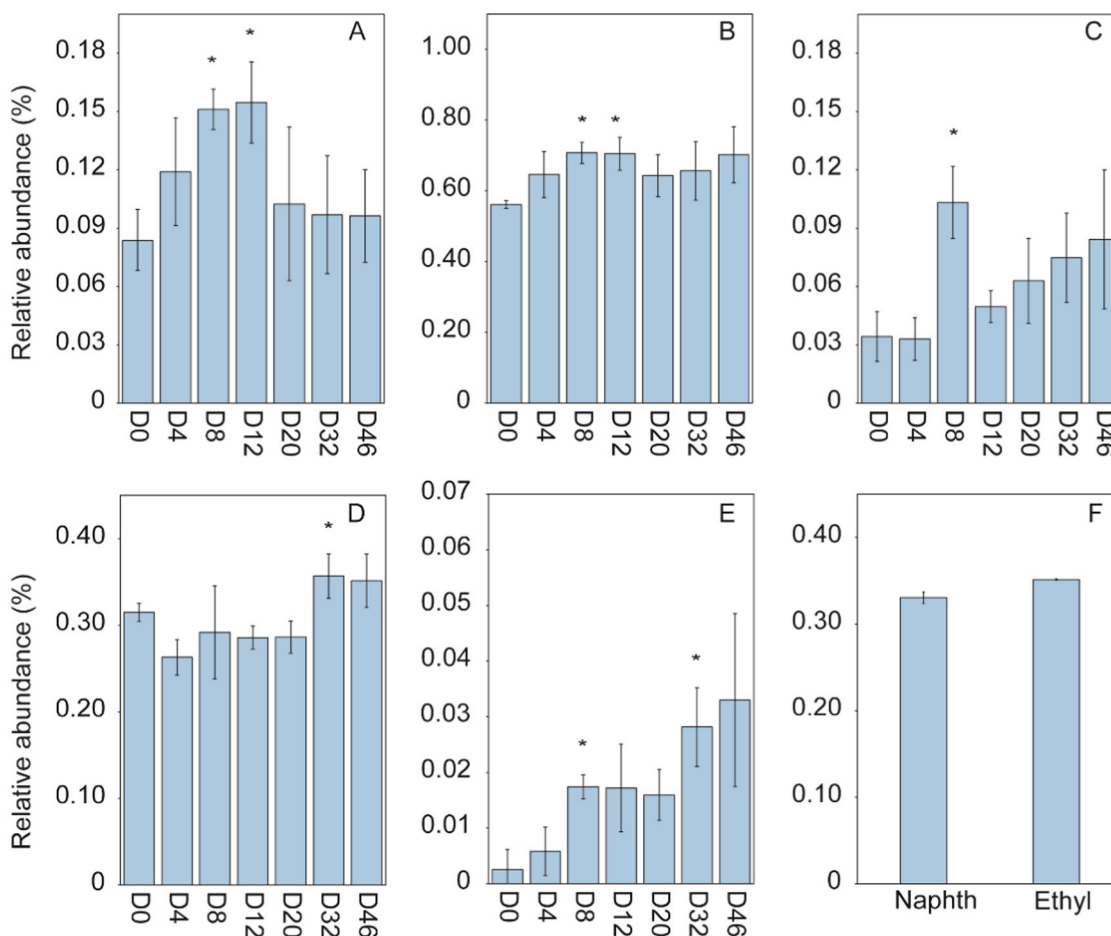


**Fig. 4.** Relative abundances of predicted pathways involved in the degradation of xenobiotics during HTC. (A) Chlorocyclohexane and chlorobenzene. (B) Chloroalkane and chloroalkene. (C) Xylene. (D) Benzoate. (E) Polycyclic aromatic hydrocarbon (PAHs). (F) Naphthalene (Naphth) and ethylbenzene (Ethyl). Asterisks indicate significant differences compared to D0 (ANOVA analysis followed by post hoc Dunnett's test,  $P < 0.05$ ).

per sample). The bacterial community composition exhibited significant temporal variations during HTC (Fig. 3A). At phylum level, Firmicutes was the dominant phylum throughout the composting, accounting for 67–82 % of all samples. The abundance of other dominant phyla, Actinobacteria, Chloroflexi and Gemmatimonadota were observed to increase during the composting process except a slight decrease on D20. In contrast, the abundance of Proteobacteria decreased from 17 % on D0 to 3 % on D46. At genus level, *Jeotgalicoccus* and *Psychrobacter* were dominant on D0, accounting for 30 % and 29 % of all genera, respectively. While, *Salinicoccus* was the dominant genus, with relative abundance increased from 2.7 % to 40.1 % after 46 days. The relative abundance of some genera increased at specific stages, e.g., *Sporosarcina* on D4 and D12 when temperature of the compost peaked at 90 °C. Additionally, *Bacillus* and two Actinobacteria genera of uncultured *Actinomarinales* and *Microtrichales* were also dominant (mean relative abundance > 3 %) in hyperthermophilic compost.

According to previous studies, totally 16 genera associated with antibiotic degradation were identified and enriched during the mid phase (Fig. 3B, and Table S3). Bacterial alpha diversity significantly increased from D0 to D8 (Fig. 3C). PCoA analysis (Adonis,  $R^2 = 0.5830$ ,  $P < 0.001$ ) further indicated significant shift in the bacterial community structures during the process (Fig. 3D).

Correlation-based network analysis obtained from the complete dataset of 22 samples revealed distinct co-occurrence patterns in composting bacterial community (Fig. S5). The Zi-Pi plot identified 18 keystone nodes within the ecological network (Fig. 3E). The 9 module hubs were assigned to 3 phyla, primarily belonging to Actinobacteria.

ASV10, assigned as *Bacillus*, was the most abundant hub node during each heating phase (D4, D12, D20, Fig. 3F). Most of the connectors belongs to Firmicutes but varied at class level (Fig. 3F), many of which were reported with biodegradation ability and were extreme-tolerant (Table S4).

In all, 172 KEGG pathways and 6 functional modules were obtained in the functional prediction analysis, with the metabolism category being the dominant pathway. Functions related to xenobiotic biodegradation and metabolism were significantly enriched (Dunnett's test,  $P < 0.05$ ) during composting (Fig. 4, and Table S5). Compared to D0, four pathways referring to the degradation of chlorocyclohexane and chlorobenzene, chloroalkane and chloroalkene, xylene, and polycyclic aromatic hydrocarbon (PAHs) were enriched after 8 days. Functions involved in PAHs degradation, along with benzoate degradation, were significantly enriched at the middle-late stage of composting. Pathways involving naphthalene and ethylbenzene degradation were detected on D20, implying an increase in bacterial metabolism potentials during composting. Additionally, pathways involving enzymes that participate in drug metabolism and the biotransformation of xenobiotics via cytochrome P450 were also identified throughout the composting process.

Network analysis (Fig. 5A) identified 65 genera closely correlated with ARGs ( $r > 0.8$ ,  $P < 0.01$ ) during HTC. Both the bacterial genera and associated ARGs exhibited a decreasing trend in abundance throughout the process (Fig. 5B). The dominant bacterial taxa were primarily Firmicutes and Actinobacteria. *Jeotgalicoccus* was the most abundant ARG-associated genera related with a MLSB resistant gene (*inuA*). It was also one of the top 10 abundant genera in composting

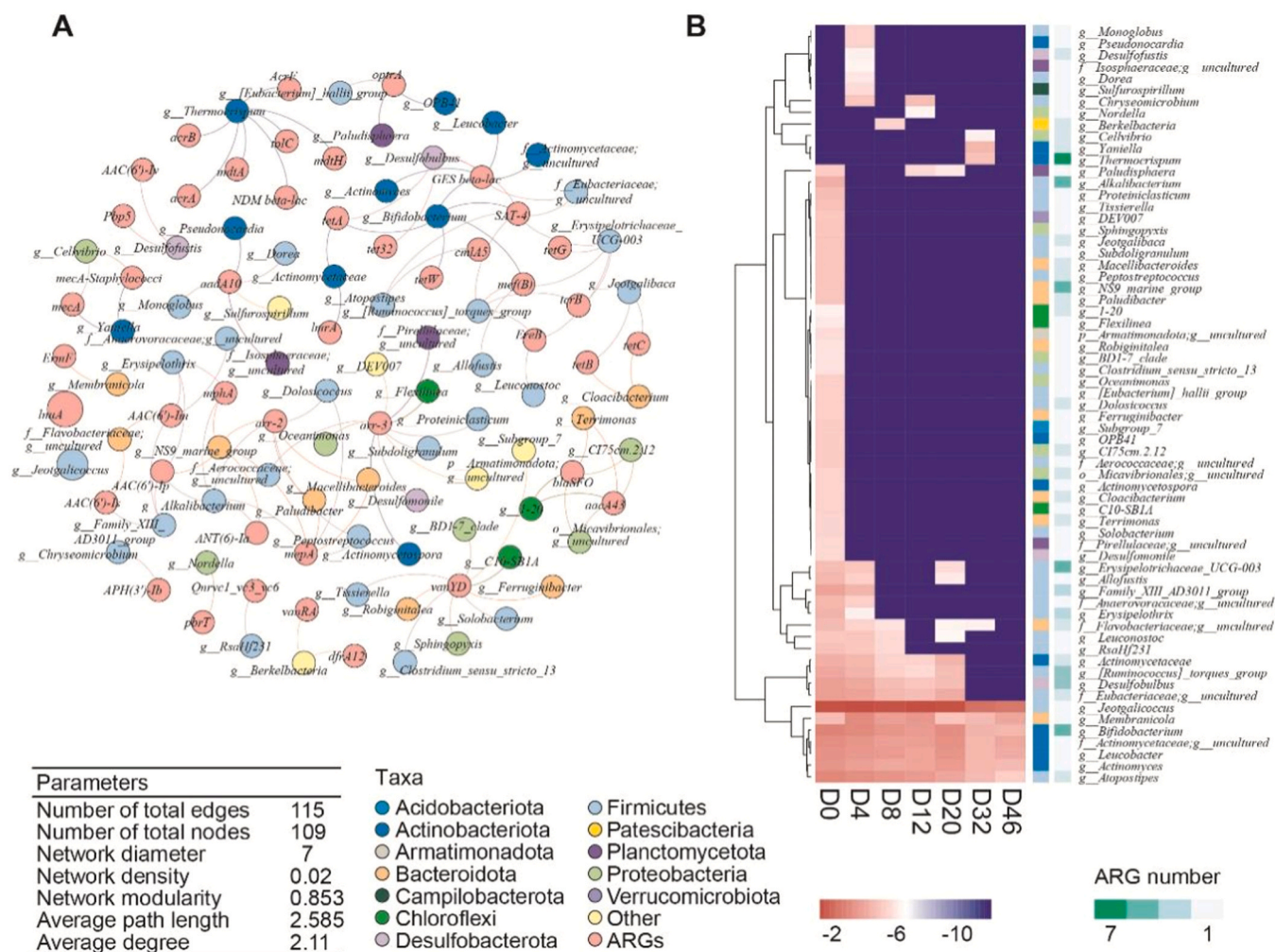


**Fig. 5.** (A) Co-occurrence network of ARGs and bacterial taxa based on the complete dataset from D0 to D46. Circle sizes represent the average relative abundance of ARGs and bacterial genera, while colors indicate different bacterial phyla. (B) Changes in relative abundances of ARG-associated genera during composting. The term "ARG number" indicates the count of different types of ARGs that showed significant correlations with bacteria. Abundance values were log<sub>10</sub> transformed.

bacteria. *Bifidobacterium*, *Desulfobulbus*, and *Ruminococcus\_torques\_group* had significant correlations with more than four types of ARGs, implying potential horizontal gene transfer according to the observed overlap in ARG types. A majority of genera that were associated with one or two types of ARGs diminished after the early phase.

### 3.5. Effects of abiotic and biotic factors on ARGs variation

Correlation analysis (Fig. 6A) revealed significant correlation between profiles of bacterial communities (based on ASV abundances) and ARG profiles (based on relative abundances) with moisture, organic matter, NH<sub>4</sub>-N content, and FQ concentrations, and between MGE profiles and moisture and NH<sub>4</sub>-N content (Mantel test,  $r > 0.2$ ,  $P < 0.01$ ). Additionally, bacterial composition exhibited significant correlations with temperature ( $P < 0.05$ ). RDA analysis was employed to discern the effects of factors and guide index selection for subsequent SEM analysis. NH<sub>4</sub>-N content emerged as one of the factors affecting ARG profiles, followed by antibiotic residues, relative abundance of transposases and Actinobacteria (Fig. 6B).

SEM analysis (Fig. 6C) indicated that composting temperature had no statistically significant effect on either composting properties ( $P = 0.078$ ) or antibiotic residue concentrations ( $P = 0.107$ ). However, it played a crucial role in shaping bacterial community compositions, which was also significantly associated with antibiotic concentrations.

Although direct effects of environmental factors on the ARGs profile were not observed, composting properties demonstrated a positive impact on the MGE abundance. Both biotic factors strongly influenced the abundance of ARGs. Specifically, the bacterial composition exhibited significant negative effect on ARG abundance, whereas the abundance of MGEs was positively correlated with ARG abundance. In summary, these results suggested that temperature and other physico-chemical properties of HTC directly affected the bacterial composition and MGE abundance, and consequently contributing to the attenuation of ARGs.

## 4. Discussion

In this study, we investigated the performance of plant-scale HTC for treating antibiotic-contaminated sewage sludge. The final product of HTC was phytotoxicity-free and exhibited high maturity. A comprehensive assessment demonstrated significant reduction of antibiotic residues, ARGs and human pathogens, suggesting that the HTC process was efficient in contaminant elimination and promise for safe recycling of sludge.

Various residual antibiotics were observed in the initial mixture (Fig. 1B), attributed to their low biodegradability and high adsorption in sludge [35,36]. Our hyperthermophilic composting demonstrated efficient elimination of four classes of antibiotics at relatively low

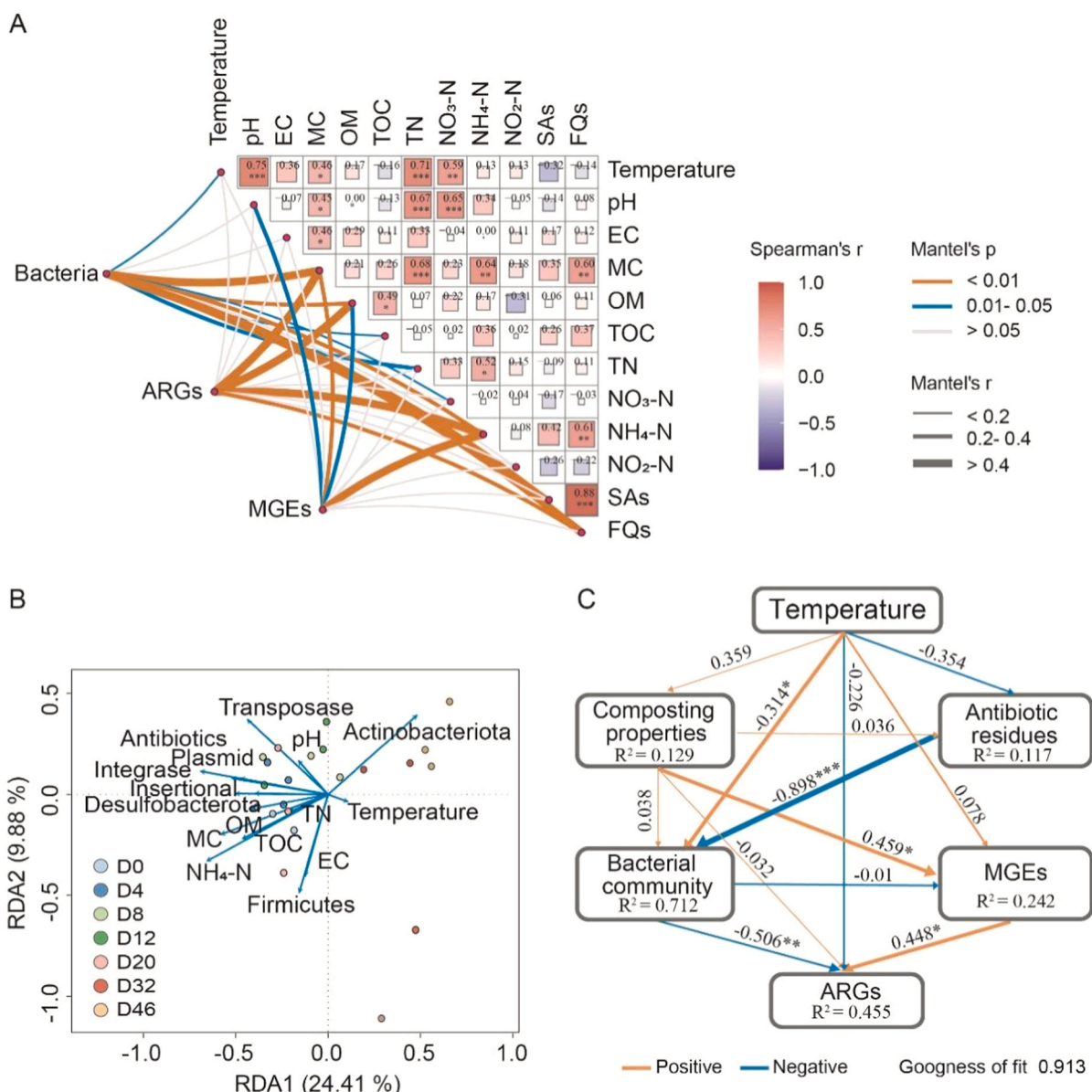


**Fig. 6.** Abiotic and biotic drivers of ARGs variation in HTC. (A) Correlations of ARG profiles with bacterial community, MGEs profiles, and composting variables. Composting variables include composting temperature, pH, EC, moisture (MC), the contents of organic matter (OM), total organic C (TOC), total nitrogen (TN), nitrate (NO<sub>3</sub>-N), nitrite (NO<sub>2</sub>-N), ammonium (NH<sub>4</sub>-N), as well as the concentrations of sulfonamides (SAs) and fluoroquinolones (FQs) antibiotics. Pairwise correlations of the variables are depicted with a color gradient denoting Pearson's correlation coefficient. Edge width represents the Mantel's r value, and the edge color denotes statistical significance. (B) Redundancy analysis illustrating the relationship among abiotic environmental conditions, bacterial communities, MGEs, and ARGs. (C) SEMs describing the relationships between composting temperature, filtered composting variables (the significant explanatory variables identified in RDA analysis), bacterial community composition, and MGE abundance on the abundance of ARGs during composting. Arrow widths correspond to the significance of the effects, and numbers indicate the standard path coefficients. R<sup>2</sup> represents the proportion of explained variation of every dependent factor after 999 bootstrap replicates. All abundances used in the statistical analysis are expressed as relative abundances.

concentrations, showcasing promising potential for low-level antibiotic removal. Moreover, despite previously recorded diminished capacities after compost enlargement [37,38], most antibiotics like SAs and CPs were completely removed within 12 days in our composting (Fig. 1C), surpassing the efficacy of conventional composting on pilot and industrial scales ranging from 30 % to 70 % in a month [39,40]. The removal of FQs was slower than SAs and CPs during HTC, suggesting FQs is more recalcitrant than SAs and CPs. The persistence of FQs in final product have been reported in conventional composting [41], while FQs residue was not detected in our composting, highlighting the potential of HTC in the removal of recalcitrant antibiotics.

High temperatures can influence antibiotic removal during

composting through various mechanisms, including thermal decomposition and volatilization, and microbial transformation. Previous studies have demonstrated that SAs and FQs exhibit high thermal stability [42], suggesting that thermal decomposition might not significantly contribute to the removal of the major antibiotics in our compost. Other than the potential physical influences of high temperature and artificial turning, our study revealed the pivotal role of microbial biodegradation in antibiotic elimination during HTC. Numerous bacteria potentially involved in antibiotic transformation and degradation were detected in samples (Fig. 3B). Thermotolerant Firmicutes, such as *Bacillus* and *Geobacillus*, have been previously reported with the ability to degrade antibiotics under extreme conditions [43,44]. These

antibiotic-degrading candidates exhibited significant enrichment aligned with antibiotic dissipation, especially on D20, coinciding with the peak removal rate of OFC. Besides, some dominant genera (Fig. 3A) in composting exhibit versatile potential for degrading complex organic contaminants. Some of these pathways are closely associated with antibiotic transformation and degradation. For instance, hydroxylation of nitrotoluene and SAs [45], dehalogenation of chlorobenzene and CAP [46], as well as cleavage of aromatic ring and heterocyclic ring in most PAHs and antibiotics [47]. This suggested the microbial communities involved in composting are equipped with versatile enzymatic machinery capable of degrading a broad spectrum of organic pollutants, implying the role of biodegradation in antibiotic elimination (Fig. 4).

Diverse ARGs and MGEs presented at a high absolute abundance in the initial mixture (Fig. 2), implying a crucial risk of ARGs enrichment and diffusion. Previous studies have indicated that moderate thermophilic composting (approximately 55–70 °C) did not effectively solve this issue. Liao et al. [9] indicated that the removal rates of ARGs and MGEs in conventional sludge composting were only 67 % and 58 %. Our previous lab-scale research even revealed a significantly increase in the copy number of ARGs after sludge composting [3]. Enrichment of ARGs was also recorded in an aerobic composting with external heating and kept at 55 °C during the heating phase [48]. Analysis of a broader range of targeted genes using high-throughput quantitative technology, nearly complete elimination of ARGs and MGEs (with removal rate up to 98.8 % and 88.1 % respectively) were achieved after our HTC, comparable with previous studies [9,10], suggesting the effectiveness of HTC in decreasing the risk of ARGs dissemination from sludge.

The shift in the compost microbiome was suggested as a major driver for the variation of ARG patterns. The absolute abundance of bacteria showed a downward trend during composting, positively correlated with that of ARGs (Fig. 2A). The influence of modified thermophilic condition, i.e., elevated temperature and prolonged thermophilic stage, on ARG elimination is noteworthy. The declined bacterial abundance could be attributed to the adverse effects of elevated composting temperature on initial sludge microbiota, including those carrying ARGs. Accordingly, a noticeable reduction in ARG-associated bacteria was observed after the initial heating stage (D4, Fig. 5B), directly leading to a significant decrease in the ARGs (Fig. 2).

In addition, the antibiotic concentration was significantly correlated with the abundance of ARGs (Fig. 6A, and Table S2), suggesting that the degradation of antibiotics during composting would weaken the selective pressure to bacterial communities and thus partially contribute to the decrease of ARGs, particularly those conferring resistance to FQs, SAs and MLSB.

Besides, the RDA analysis indicated potential contribution of NH<sub>4</sub>-N content in shaping the ARG profiles (Fig. 6B). Given the significant correlation between NH<sub>4</sub>-N content, the composition of the bacterial community, and the antibiotic resistome pattern (Fig. 6A), we infer that ammonia conversion could also be crucial in driving the changes of bacterial communities, which in turn influences the ARGs and MGEs during HTC. Moreover, the reduction in the abundance of potential ARG-hosts and MGEs could further decrease the horizontal transfer potential of ARGs [49].

## 5. Conclusion

In this study, we demonstrated the efficiency of HTC in removing antibiotic residues and antibiotic resistome from plant-scale sludge waste, producing high-quality fertilizers. The reduction of ARGs was primarily attributed to the decline in ARG-associated bacteria owing to elevated temperature and prolonged thermophilic duration. Furthermore, our results underscore the crucial role of bacterial metabolism in the elimination of antibiotics during HTC. This study expands the understanding of the mechanisms underlying the elimination of antibiotics and ARGs using HTC and confirms its feasibility in sludge cleaning and recycling.

## Environmental implication

Antimicrobial resistance (AMR) poses a global crisis, with sewage sludge identified as a key reservoir for antibiotic residues and resistance genes (ARGs). Traditional composting methods may exacerbate these concerns by potentially disseminating antibiotics and ARGs into ecosystem upon land application. Our study investigates hyperthermophilic composting as a promising solution. Findings reveal complete antibiotic removal, pathogen elimination, and significant reduction of ARGs and mobile genetic elements after composting. By elucidating the roles of biodegradation and high-temperature selection, our research enhances understanding of the underlying mechanisms of hyperthermophilic composting in eliminating antibiotics and ARGs.

## CRedit authorship contribution statement

**Jian-Qiang Su:** Writing – review & editing, Supervision, Funding acquisition, Conceptualization. **Qiang Pu:** Software, Investigation. **Xin-Li An:** Methodology, Formal analysis. **Qian Xiang:** Writing – review & editing, Methodology, Formal analysis. **Yan-Yan Zhou:** Writing – review & editing, Project administration, Investigation, Formal analysis, Data curation. **Ting Pan:** Writing – review & editing, Writing – original draft, Visualization, Software, Methodology, Investigation, Formal analysis, Data curation.

## Declaration of Competing Interest

The authors declare that they have no known competing financial interests or personal relationships that could have appeared to influence the work reported in this paper.

## Data availability

Data will be made available on request.

## Acknowledgements

This work was supported by the National Natural Science Foundation of China (42161134002) and the National Key Research and Development Plan (2020YFC1806902). We thank Xiang Zheng for the sample collection, Jia-Zhi Ding for assisting the DNA extraction, Bing Hong, Min Zhou, and Juan Li for guidance on antibiotic analysis, Xin-Yuan Zhou, Hu Liao, and Zu-Fei Xiao for assistance with statistical analysis, Yi-Jia Tang, Xiao-Xuan Su, and Fu-Yi Huang for their valuable help with manuscript revision.

## Appendix A. Supporting information

Supplementary data associated with this article can be found in the online version at [doi:10.1016/j.jhazmat.2024.135525](https://doi.org/10.1016/j.jhazmat.2024.135525).

## References

- [1] Hernando-Amado, S., Coque, T.M., Baquero, F., Martinez, J.L., 2019. Defining and combating antibiotic resistance from One Health and Global Health perspectives. *Nat Microbiol* 4 (9), 1432–1442. <https://doi.org/10.1038/s41564-019-0503-9>.
- [2] van Holst, S., van Holst, S., Schmitt, H., van der Zaan, B.M., Gerritsen, H.W., Rijnaarts, H.H.M., 2020. et al. Fate of antibiotics and antibiotic resistance genes during conventional and additional treatment technologies in wastewater treatment plants. *Sci Total Environ* 741, 140199. <https://doi.org/10.1016/j.scitotenv.2020.140199>.
- [3] Su, J.Q., Wei, B., Ou-Yang, W.Y., Huang, F.Y., Zhao, Y., Xu, H.J., et al., 2015. Antibiotic resistome and its association with bacterial communities during sewage sludge composting. *Environ Sci Technol* 49 (12), 7356–7363. <https://doi.org/10.1021/acs.est.5b01012>.
- [4] Zhao, C., Xin, L., Xu, X., Qin, Y., Wu, W., 2022. Dynamics of antibiotics and antibiotic resistance genes in four types of kitchen waste composting processes. *J Hazard Mater* (424(Pt C)), 127526. <https://doi.org/10.1016/j.jhazmat.2021.127526>.

- [5] Wu, J., Wang, J., Li, Z., Guo, S., Li, K., Xu, P., et al., 2022. Antibiotics and antibiotic resistance genes in agricultural soils: a systematic analysis. *Crit Rev Environ Sci Technol* 53 (7), 847–864. <https://doi.org/10.1080/10643389.2022.2094693>.
- [6] Zhang, J., Sui, Q., Tong, J., Zhong, H., Wang, Y., Chen, M., et al., 2018. Soil types influence the fate of antibiotic-resistant bacteria and antibiotic resistance genes following the land application of sludge composts. *Environ Int* 118, 34–43. <https://doi.org/10.1016/j.envint.2018.05.029>.
- [7] Wang, S., Wu, Y., 2021. Hyperthermophilic composting technology for organic solid waste treatment: Recent research advances and trends. *Processes* 9 (4). <https://doi.org/10.3390/pr9040675>.
- [8] Oshima, T., Moriya, T., 2008. A preliminary analysis of microbial and biochemical properties of high-temperature compost. *Ann N Y Acad Sci* 1125, 338–344. <https://doi.org/10.1196/annals.1419.012>.
- [9] Liao, H., Lu, X., Rensing, C., Friman, V.P., Geisen, S., Chen, Z., et al., 2018. Hyperthermophilic composting accelerates the removal of antibiotic resistance genes and mobile genetic elements in sewage sludge. *Environ Sci Technol* 52 (1), 266–276. <https://doi.org/10.1021/acs.est.7b04483>.
- [10] Liao, H., Zhao, Q., Cui, P., Chen, Z., Yu, Z., Geisen, S., et al., 2019. Efficient reduction of antibiotic residues and associated resistance genes in tylosin antibiotic fermentation waste using hyperthermophilic composting. *Environ Int* 133. <https://doi.org/10.1016/j.envint.2019.105203>.
- [11] Manai, C.M., Rocha, J., Scaccia, N., Marano, R., Radu, E., Biancullo, F., et al., 2018. Antibiotic resistance in wastewater treatment plants: tackling the black box. *Environ Int* 115, 312–324. <https://doi.org/10.1016/j.envint.2018.03.044>.
- [12] Lin, H., Zhang, J., Chen, H., Wang, J., Sun, W., Zhang, X., et al., 2017. Effect of temperature on sulfonamide antibiotics degradation, and on antibiotic resistance determinants and hosts in animal manures. *Sci Total Environ* 607, 725–732. <https://doi.org/10.1016/j.scitotenv.2017.07.057>.
- [13] Zhang, J., Bao, Y., Jiang, Y., Liu, H.T., Xi, B.D., Wang, D.Q., 2019. Removal and dissipation pathway of typical fluoroquinolones in sewage sludge during aerobic composting. *Waste Manag* 95, 450–457. <https://doi.org/10.1016/j.wasman.2019.06.036>.
- [14] Sun, P., Liu, B., Ahmed, I., Yang, J., Zhang, B., 2022. Composting effect and antibiotic removal under a new temperature control strategy. *Waste Manag* 153, 89–98. <https://doi.org/10.1016/j.wasman.2022.08.025>.
- [15] Wei, Y., Li, J., Shi, D., Liu, G., Zhao, Y., Shimaoka, T., 2017. Environmental challenges impeding the composting of biodegradable municipal solid waste: a critical review. *Resour Conserv Recycl* 122, 51–65. <https://doi.org/10.1016/j.resconrec.2017.01.024>.
- [16] Bernal, M.P., Alburquerque, J.A., Moral, R., 2009. Composting of animal manures and chemical criteria for compost maturity assessment. A review. *Bioresour Technol* 100 (22), 5444–5453. <https://doi.org/10.1016/j.biortech.2008.11.027>.
- [17] Cernava, T., Erlacher, A., Soh, J., Sensen, C.W., Grube, M., Berg, G., 2019. *Enterobacteriaceae* dominate the core microbiome and contribute to the resistome of arugula (*Eruca sativa* Mill.). *Microbiome* 7 (1), 13. <https://doi.org/10.1186/s40168-019-0624-7>.
- [18] Sadeghi, S., Nikaeen, M., Mohammadi, F., Hossein Nafez, A., Gholipour, S., Shamsizadeh, Z., et al., 2022. Microbial characteristics of municipal solid waste compost: occupational and public health risks from surface applied compost. *Waste Manag* 144, 98–105. <https://doi.org/10.1016/j.wasman.2022.03.012>.
- [19] Liao, H., Chen, Z., Yu, Z., Lu, X., Wang, Y., Zhou, S., 2017. Development of hyperthermophilic aerobic composting and its engineering applications in organic solid wastes. *Fujian Agric Univ* 46 (4), 439–444. [https://doi.org/10.13323/j.cnki.j.fafu\(nat.sci.\).2017.04.014](https://doi.org/10.13323/j.cnki.j.fafu(nat.sci.).2017.04.014).
- [20] Cao, Y., Chang, Z.Z., Huang, H.Y., Xu, Y.D., Li, C.F., Wu, H.S., 2015. Effect of compost inoculation on pig manure composting. *Transactions of the Chinese Society of Agricultural Engineering (Transactions of the CSAE)* 31 (21), 220–226. <https://doi.org/10.11975/j.issn.1002-6819.2015.21.029>.
- [21] Zhou, G.W., Yang, X.R., Li, H., Marshall, C.W., Zheng, B.X., Yan, Y., Su, J.Q., Zhu, Y.G., 2016. Electron Shuttles Enhance Anaerobic Ammonium Oxidation Coupled to Iron(III) Reduction. *Environ Sci Technol* 50 (17), 9298–9307. <https://doi.org/10.1021/acs.est.6b02077>.
- [22] Guo, R., Li, G., Jiang, T., Schuchardt, F., Chen, T., Zhao, Y., et al., 2012. Effect of aeration rate, C/N ratio and moisture content on the stability and maturity of compost. *Bioresour Technol* 112, 171–178. <https://doi.org/10.1016/j.biortech.2012.02.099>.
- [23] Zhou, M., Yu, S., Hong, B., Li, J., Han, H., Qie, G., 2021. Antibiotics control in aquaculture requires more than antibiotic-free feeds: A tilapia farming case. *Environ Pollut* (268(Pt B)), 115854. <https://doi.org/10.1016/j.envpol.2020.115854>.
- [24] An, X.L., Wang, J.Y., Pu, Q., Li, H., Pan, T., Li, H.Q., et al., 2020. High-throughput diagnosis of human pathogens and fecal contamination in marine recreational water. *Environ Res* 190, 109982. <https://doi.org/10.1016/j.envres.2020.109982>.
- [25] Stedtfeld, R.D., Guo, X., Stedtfeld, T.M., Sheng, H., Williams, M.R., Hauschild, K., et al., 2018. Primer set 2.0 for highly parallel qPCR array targeting antibiotic resistance genes and mobile genetic elements. *FEMS Microbiol Ecol* 94 (9). <https://doi.org/10.1093/femsec/fiy130>.
- [26] Zhu, D., Ding, J., Yin, Y., Ke, X., O'Connor, P., Zhu, Y.-G., 2020. Effects of earthworms on the microbiomes and antibiotic resistomes of detritus fauna and phyllospheres. *Environ Sci Technol* 54 (10), 6000–6008. <https://doi.org/10.1021/acs.est.9b04500>.
- [27] Zhou, J., Deng, Y., Shen, L., Wen, C., Yan, Q., Ning, D., et al., 2016. Temperature mediates continental-scale diversity of microbes in forest soils. *Nat Commun* 7, 12083. <https://doi.org/10.1038/ncomms12083>.
- [28] Callahan, B.J., McMurdie, P.J., Rosen, M.J., Han, A.W., Johnson, A.J., Holmes, S.P., 2016. DADA2: high-resolution sample inference from Illumina amplicon data. *Nat Methods* 13 (7), 581–583. <https://doi.org/10.1038/nmeth.3869>.
- [29] Douglas, G.M., Maffei, V.J., Zaneveld, J.R., Yurgel, S.N., Brown, J.R., Taylor, C.M., et al., 2020. PICRUSt2 for prediction of metagenome functions. *Nat Biotechnol* 38 (6), 685–688. <https://doi.org/10.1038/s41587-020-0548-6>.
- [30] Dixon, P., 2003. VEGAN, a package of R functions for community ecology. *J Veg Sci* 14 (6). <https://doi.org/10.1111/j.1654-1103.2003.tb02228.x>.
- [31] Liu, C., Cui, Y., Li, X., Yao, M., 2021. *microeco*: an R package for data mining in microbial community ecology. *FEMS Microbiol Ecol* 97 (2). <https://doi.org/10.1093/femsec/iaa255>.
- [32] Zhao, S., Schmidt, S., Gao, H., Li, T., Chen, X., Hou, Y., et al., 2022. A precision compost strategy aligning composts and application methods with target crops and growth environments can increase global food production. *Nat Food* 3 (9), 741–752. <https://doi.org/10.1038/s43016-022-00584-x>.
- [33] Zhang, J., Chen, G., Sun, H., Zhou, S., Zou, G., 2016. Straw biochar hastens organic matter degradation and produces nutrient-rich compost. *Bioresour Technol* 200, 876–883. <https://doi.org/10.1016/j.biortech.2015.11.016>.
- [34] Estrella-Gonzalez, M.J., Suarez-Estrella, F., Jurado, M.M., Lopez, M.J., Lopez-Gonzalez, J.A., Siles-Castellano, A.B., et al., 2020. Uncovering new indicators to predict stability, maturity and biodiversity of compost on an industrial scale. *Bioresour Technol* 313, 123557. <https://doi.org/10.1016/j.biortech.2020.123557>.
- [35] Oberoi, A.S., Jia, Y., Zhang, H., Khanal, S.K., Lu, H., 2019. Insights into the fate and removal of antibiotics in engineered biological treatment systems: A critical review. *Environ Sci Technol* 53 (13), 7234–7264. <https://doi.org/10.1021/acs.est.9b01131>.
- [36] Wang, L., Qiang, Z., Li, Y., Ben, W., 2017. An insight into the removal of fluoroquinolones in activated sludge process: Sorption and biodegradation characteristics. *J Environ Sci* 56, 263–271. <https://doi.org/10.1016/j.jes.2016.10.006>.
- [37] Chen, Z., Wang, Y., Wen, Q., Zhang, S., Yang, L., 2016. Feasibility study of recycling cephalosporin C fermentation dregs using co-composting process with activated sludge as co-substrate. *Environ Technol* 37 (17), 2222–2230. <https://doi.org/10.1080/09593330.2016.1146340>.
- [38] Mitchell, S.M., Ullman, J.L., Bary, A., Cogger, C.G., Teel, A.L., Watts, R.J., 2015. Antibiotic degradation during thermophilic composting. *Water Air Soil Pollut* 226 (2). <https://doi.org/10.1007/s11270-014-2288-z>.
- [39] Cessna, A.J., Larney, F.J., Kuchta, S.L., Hao, X., Entz, T., Topp, E., et al., 2011. Veterinary antimicrobials in feedlot manure: dissipation during composting and effects on composting processes. *J Environ Qual* 40 (1), 188–198. <https://doi.org/10.2134/jeq2010.0079>.
- [40] Serpillanges, N., Haudin, C.S., Bourdat-Deschamps, M., Bernet, N., Serre, V., Danel, A., et al., 2020. Process type is the key driver of the fate of organic micropollutants during industrial scale treatment of organic wastes. *Sci Total Environ* 734, 139108. <https://doi.org/10.1016/j.scitotenv.2020.139108>.
- [41] Khadra, A., Ezzari, A., Merlina, G., Capdeville, M.J., Budzinski, H., Hamdi, H., et al., 2019. Fate of antibiotics present in a primary sludge of WWTP during their co-composting with palm wastes. *Waste Manag* 84, 13–19. <https://doi.org/10.1016/j.wasman.2018.11.009>.
- [42] Jie, L., Lanjia, P., Guangwei, Y., Futian, Y., Shengyu, X., Yin, W., 2017. Pyrolysis characteristics and kinetics analysis of several antibiotics in sludge. *Chin J Environ Eng* 11 (9), 5213–5219. <https://doi.org/10.12030/j.cjee.201609031>.
- [43] Dong, Z., Yan, X., Wang, J., Zhu, L., Wang, J., Li, C., et al., 2022. Mechanism for biodegradation of sulfamethazine by *Bacillus cereus* H38. *Sci Total Environ* 809, 152237. <https://doi.org/10.1016/j.scitotenv.2021.152237>.
- [44] Pan, L.J., Tang, X.D., Li, C.X., Yu, G.W., Wang, Y., 2017. Biodegradation of sulfamethazine by an isolated thermophile-*Geobacillus* sp. S-07. *World J Microbiol Biotechnol* 33 (5), 85. <https://doi.org/10.1007/s11274-017-2245-2>.
- [45] Hu, J., Li, X., Liu, F., Fu, W., Lin, L., Li, B., 2022. Comparison of chemical and biological degradation of sulfonamides: Solving the mystery of sulfonamide transformation. *J Hazard Mater* (424(Pt D)), 127661. <https://doi.org/10.1016/j.jhazmat.2021.127661>.
- [46] Gao, Y., Cheng, H., Song, Q., Huang, J., Liu, J., Pan, D., et al., 2024. Characteristics and catalytic mechanism of a novel multifunctional oxidase, CpmO, for chloramphenicol degradation from *Sphingobium* sp. WTD-1. *J Hazard Mater* 465. <https://doi.org/10.1016/j.jhazmat.2023.133348>.
- [47] Wu, T., Guo, S.Z., Zhu, H.Z., Yan, L., Liu, Z.P., Li, D.F., et al., 2023. The sulfonamide-resistance dihydropteroate synthase gene is crucial for efficient biodegradation of sulfamethoxazole by Paenarthrobacter species. *Appl Microbiol Biotechnol* 107 (18), 5813–5827. <https://doi.org/10.1007/s00253-023-12679-x>.
- [48] Chen, Z., Fu, Q., Wen, Q., Wu, Y., Bao, H., Guo, J., 2022. Microbial community competition rather than high-temperature predominates ARGs elimination in swine manure composting. *J Hazard Mater* 423. <https://doi.org/10.1016/j.jhazmat.2021.127149>.
- [49] Ma, L., Xia, Y., Li, B., Yang, Y., Li, L.G., Tiedje, J.M., et al., 2016. Metagenomic assembly reveals hosts of antibiotic resistance genes and the shared resistome in pig, chicken, and human feces. *Environ Sci Technol* 50 (1), 420–427. <https://doi.org/10.1021/acs.est.5b03522>.